CHINESE OPTICS LETTERS

Vol. 20, No. 2 | February 2022

Optical limiting performances of transitional metal dichalcogenides MX_2 (M = V, Nb, Ta; X = S, Se) with ultralow initial threshold and optical limiting threshold

Chenglu Liang (梁成露)[1,†], Enze Wang (王恩泽)[1,†], Xian Li (李 仙)[1], Jing Wang (汪 静)[1], Yijun Liu (刘毅俊)[1], Binyi Chen (陈斌艺)[1], Hongxiang Chen (陈洪祥)[1,2*], Yang Liu (刘 洋)[1,2,3,4**], and Xiangfang Peng (彭响方)[1]

[1] Department of Materials Science and Engineering, Fujian University of Technology, Fuzhou 350108, China

[2] Center for Advanced Energy and Functional Materials, Fujian University of Technology, Fuzhou 350108, China

[3] State Key Laboratory of Polymer Materials Engineering, Sichuan University, Chengdu 610207, China

[4] State Key Laboratory of Materials Processing and Die & Mould Technology, Huazhong University of Science and Technology, Wuhan 430074, China

*Corresponding author: lost0512@126.com

**Corresponding author: nxly18@163.com

Received June 30, 2021 | Accepted August 17, 2021 | Posted Online October 8, 2021

The optical limiting performances of few-layer transitional metal dichalcogenides (TMDs) nanosheets in the VB group (VS_2, VSe_2, NbS_2, $NbSe_2$, TaS_2, and $TaSe_2$) were systematically investigated for the first time, to the best of our knowledge. It was found that these TMDs nanosheets showed a normalized transmittance in the range of 20%–40% at the input energy of 1.28 GW/cm^2. Ultralow initial threshold F_S (0.05–0.10 J/cm^2) and optical limiting threshold F_{OL} (0.82–2.23 J/cm^2) were achieved in the TMDs nanosheets, which surpassed most of the optical limiting materials. This work showed the potential of TMDs beyond MoS_2 in optical limiting field.

Keywords: optical limiting; transitional metal dichalcogenide; initial threshold; optical limiting threshold.
DOI: 10.3788/COL202220.021901

1. Introduction

With the wide application of high-intensity laser and related electronic equipments in sensor, communication, military, and medical fields, the development of optical limiting materials to protect optically sensitive organs or devices, such as human eyes and optical sensors, was crucial[1]. Effective optical limiting materials require the traits of low optical limiting threshold, high laser damage threshold, quick response, wide protection range of laser wavelength, and high laser protection efficiency[2]. A low optical limiting threshold is a vital parameter for effective optical limiting materials. Lasers with energy intensity reaching only a few mJ/cm^2 would cause serious damage to organs or devices. However, most of the nonlinear optical limiting materials showed feeble limiting effects when the laser intensities were lower than 100 mJ/cm^2 [3].

Transitional metal dichalcogenides (TMDs) emerged as a promising optical limiting material waiting to be explored[4]. TMDs possess a two-dimensional (2D) layered structure bonding via Van der Waals' force between the atomic layers. When the bulk TMDs were exfoliated to single/few-layer nanosheets, novel physical and chemical properties emerged in the atomic nanosheets[5,6], which endowed them with intriguing functionality that cannot be found in the bulk counterpart[7]. Among the TMDs, the VIB group metal dichalcogenides MoS_2 [7–9] and WS_2 nanosheets[10–12] were the most widely explored in optical limiting performances for high-energy lasers due to the low initial threshold, tunable nonlinear optics (NLO) responses, and unique absorption ways dependent on the number of layers. Except for metal sulfides, other chalcogenides of Mo and W like WSe_2, $MoSe_2$, and $MoTe_2$ were also reported to exhibit optical limiting performances[3,13,14]. In addition, the IVB (the fouth sub) group TMDs like ZrS_3, $ZrSe_3$, and TiS_2 were also explored as optical limiting materials[15–17]. Our previous results demonstrated that the TiS_2 nanosheets showed better optical limiting performances[17] than MoS_2 nanosheets and even better optical limiting performances than the benchmark C_{60} in terms of normalized linear transmittance. The reported TMDs in optical limiting performances are mainly VIB (the sixth sub) and IVB group TMDs, which inspired us to explore the optical limiting performances of the VB (the fifth sub) group (V, Nb, and Ta) TMDs.

In this work, the optical limiting performances of the few-layer VB group TMDs nanosheets were systematically explored

for the first time, to the best of our knowledge. The VB group TMDs (VS_2, VSe_2, NbS_2, $NbSe_2$, TaS_2, and $TaSe_2$) were synthesized via solid state sintering followed by liquid phase exfoliation (LPE) to obtain the corresponding nanosheets with the thickness less than 3 nm and lateral size over 1000 nm. All of investigated TMDs nanosheets displayed satisfying optical limiting responses with relatively low optical limiting onsets (F_S) and even lower optical limiting thresholds (F_{OL}) than the multi-wall carbon nanotubes (MWNTs) and C_{60} [18–20], among which, the VSe_2 nanosheets showed the best optical limiting performances with the ultralow F_S value of $0.05\,J/cm^2$, low F_{OL} value of $0.9\,J/cm^2$, and normalized transmittance of 0.30 at $1.28\,GW/cm^2$. This work shows the potential of TMDs beyond MoS_2 in the optical limiting field.

2. Experiments

2.1. Preparation of bulk and nanosheets 2D VS_2, VSe_2, NbS_2, $NbSe_2$, TaS_2, and $TaSe_2$

Bulk VS_2, VSe_2, NbS_2, $NbSe_2$, TaS_2, and $TaSe_2$ were synthesized via the solid state sintering method[21]. Briefly, metallic elements of V, Nb, and Ta and corresponding chalcogenides (S/Se elements) with stoichiometric ratios were vacuum sealed in the quartz tubes with an inner diameter of 8 mm and a length of 120 mm. Using halogen (I_2, $5\,mg/cm^3$) as the transfer agent, the sealed quartz tubes were heated to 550°C and maintained at this temperature for 5 h. Then, the tubes were further heated to 1000°C and maintained at this temperature for 3 days. After that, the system was cooled to room temperature, and the corresponding VS_2, VSe_2, NbS_2, $NbSe_2$, TaS_2, and $TaSe_2$ were obtained. Bulk VS_2, VSe_2, NbS_2, $NbSe_2$, TaS_2, and $TaSe_2$ were exfoliated by ultrasonication treatment. Briefly, 30 mg bulk powder was dispersed in a co-solvent of isopropyl alcohol (IPA)/H_2O (1/1, in volume), and then the dispersion was sonicated for 90 min in a water bath. The sonicated suspension was centrifuged at 2000 r/min for 30 min to remove the unexfoliated bulk sediments. The as-obtained supernate was used for optical limiting tests.

2.2. Material characterization

The thickness of the TMDs nanosheets was measured in a tapping mode by an atomic force microscope (AFM) (Dimension Icon). The UV spectrophotometer (UV-2600) was used to obtain the optical absorption spectra. The Raman spectrum was recorded by a Raman spectrometer (Invia Reflex) with laser of 532 nm as a laser source. X-ray diffraction (XRD) and X-ray photoelectron spectroscopy (XPS) were used to characterize the chemical structure of the samples.

2.3. *Z*-scan measurement

The optical limiting performances of TMDs nanosheets were investigated using an open-aperture *Z*-scan technique. The *Z*-scan technique adopted a $Nd:Y_3Al_5O_{12}$ (Nd:YAG) laser system using a 532 nm laser with a laser pulse of 7 ns (10 Hz, Brio 640, Quantel, Les Ulis, France). The input/output flux of the laser pulse was recorded by an energy meter. The suspension of samples was kept in a 2 mm glass cuvette, and the cuvette was loaded on a computer-controlled mobile platform and moved along *Z* axis through the focal plane of a 100 mm focal length lens. The waist radius in the focal plane was 23 μm, and the input energy was in the range of 20–80 μJ. The input peak light intensity at the focus was in the range of $0.32–1.28\,GW/cm^2$.

3. Results and Discussion

The RD was conducted to characterize the crystal structure of bulk TMDs and TMDs nanosheets, as shown in Fig. 1. The peaks of 2θ values at 15.5°, 32.1°, 35.9°, 44.7°, 56.8°, and 67.3° corresponded to the (001), (100), (101), (012), (110), and (200) crystal planes, respectively, which were consistent with the standard 1T-VS_2 [Inorganic Crystal Structure Database (ICSD) identification (ID) 45214][22]. The characteristic peak positions of other bulk TMDs powder matched well with their standard cards 2H- NbS_2 [Joint Committee on Powder Diffraction Standards (JCPDS) 38-1367], 1T- TaS_2 (JCPDS 02-0137), 1 T-VSe_2 (ICSD ID 45215)[22], 2 H-$NbSe_2$ (JCPDS 65-7464), and 2H-$TaSe_2$ (JCPDS 65-3657), indicating a 2D layer structure in these TMDs. After LPE, only peaks in the *c*-axis orientation, thus (001), (002), (003), and (004), remained, which proved the successful exfoliation of bulk 2D TMDs into nanosheets[23].

The direct observation of TMDs nanosheets was realized via the AFM and the AFM images are presented in Figs. 2(a)–2(f). The nanosheet structure of exfoliated TMDs was obvious. According to the height profiles [insets in Figs. 2(a)–2(f)] interpreted from corresponding AFM images, the thickness of VS_2 nanosheets was about 6 nm, and the thickness of NbS_2 was about 4 nm. Other TMDs nanosheets possessed a thickness of 1–2 nm, while all of the TMDs nanosheets showed a lateral size over 1000 nm.

An open-aperture *Z*-scan technique was used to examine the optical limiting performances of the TMDs nanosheets. A 532 nm laser source with a laser pulse of 7 ns was utilized. The normalized transmittance (the ratio of nonlinear to linear transmittance) was used to evaluate the nonlinear optical

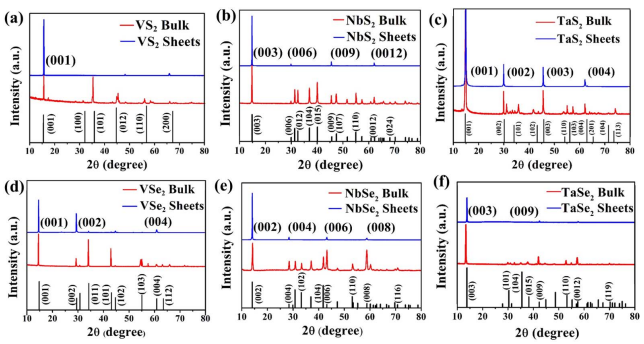

Fig. 1. XRD patterns of bulk TMDs and TMDs nanosheets. (a) VS_2; (b) NbS_2; (c) TaS_2; (d) VSe_2; (e) $NbSe_2$; (f) $TaSe_2$.

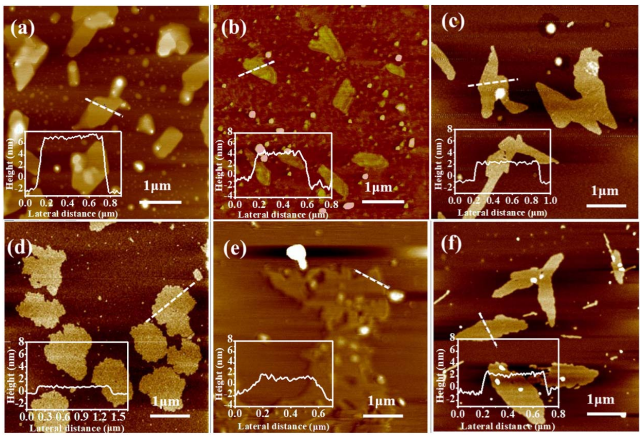

Fig. 2. AFM images and corresponding height profiles (insets) of TMDs nanosheets obtained by LPE. (a) VS_2 nanosheets; (b) NbS_2 nanosheets; (c) TaS_2 nanosheets; (d) VSe_2 nanosheets; (e) $NbSe_2$ nanosheets; (f) $TaSe_2$ nanosheets.

properties. A normalized transmittance value lower than one near the zero Z position means the existence of an optical limiting effect in materials. A lower value of normalized transmittance indicated the more enhanced optical limiting effect.

As shown in Figs. 3(a)–3(f), the normalized transmittance values of the TMDs nanosheets were lower than one near the zero Z position in the tested input energy range, exhibiting a typical optical limiting effect. With the increase in input energy, the normalized transmittance of all the tested TMDs nanosheets decreased continuously, demonstrating an enhanced limiting effect. Specifically, the normalized transmittance values of the nanosheets at $0.32\,GW/cm^2$, $0.64\,GW/cm^2$, $0.96\,GW/cm^2$, and $1.28\,GW/cm^2$ were summarized in Table 1. In addition, the normalized transmittance values of the investigated TMDs nanosheets were in the range of 0.23–0.34 at the input energy of $1.28\,GW/cm^2$.

The standard material, C_{60}, was chosen to evaluate the optical limiting performances of our materials. The nonlinear transmittance of commercial C_{60} was tested and compared with VSe_2 nanosheets, as shown in Fig. 4. The initial linear transmittances of C_{60} and VSe_2 nanosheets were unified to be 65%.

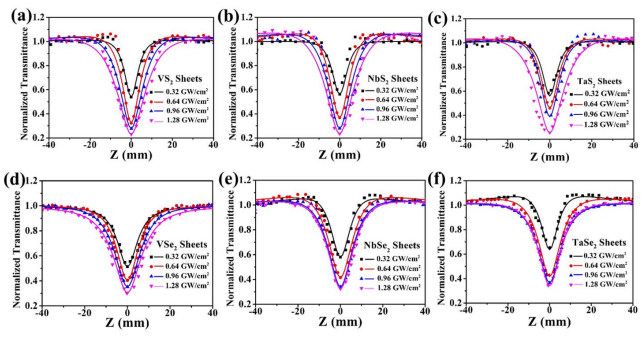

Fig. 3. Open-aperture Z-scan for (a) VS_2 nanosheets, (b) NbS_2 nanosheets, (c) TaS_2 nanosheets, (d) VSe_2 nanosheets, (e) $NbSe_2$ nanosheets, and (f) $TaSe_2$ nanosheets, with different incident laser pulse energies; solid line: theoretical fitting data.

Table 1. Normalized Transmittance Values of TMDs Nanosheets under Different Input Laser Fluences.

	Transmittance					
Fluence (GW/cm^2)	VS_2	NbS_2	TaS_2	VSe_2	$NbSe_2$	$TaSe_2$
0.32	0.53	0.56	0.55	0.51	0.58	0.64
0.64	0.32	0.36	0.45	0.40	0.41	0.42
0.96	0.28	0.28	0.38	0.35	0.34	0.37
1.28	0.23	0.23	0.25	0.30	0.32	0.34

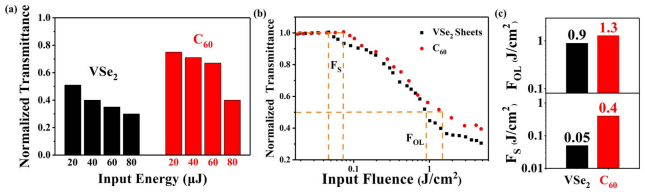

Fig. 4. Optical limiting performances of VSe_2 nanosheets and C_{60} tested at the same conditions. (a) Normalized transmittance at different input laser fluences. (b) Relationship between the normalized transmittance and the input laser fluences. (c) The F_S and F_{OL} values of C_{60} and VSe_2 nanosheets.

The summarized normalized transmittances of VSe_2 and C_{60} at different input laser fluences were shown in Fig. 4(a). As the input energy increased, the normalized transmittance of VSe_2 nanosheets decreased continuously, similar with C_{60}. However, the normalized transmittance of VSe_2 nanosheets was much lower than that of C_{60} at similar input energies, which indicated a superior optical limiting performance.

The initial threshold (F_S), defined as the incident fluence at which the optical limiting effect starts, and optical limiting threshold (F_{OL}), defined as the input fluence point at which the normalized transmittance drops to 50%, are two vital parameters for optical limiting materials. A material possessing lower F_S and F_{OL} has been pursued in optical limiting applications. The relationship between the normalized transmittance and the input laser fluences was shown in Fig. 4(b). The F_S and F_{OL} values were calculated from Fig. 4(b). The F_S and F_{OL} values of VSe_2 nanosheets were $0.05\,J/cm^2$ and $0.9\,J/cm^2$, respectively, which were much lower than that of C_{60}, as shown in Fig. 4(c). So, the VSe_2 nanosheets performed better optical limiting performance than C_{60}. The F_S and F_{OL} values of TMDs nanosheets obtained from Fig. 5(a) (the relationship between the normalized transmittance of TMDs nanosheets and the input laser fluences) are summarized in Table 2. The F_S values of the investigated TMDs nanosheets were in the range of $0.05–0.10\,J/cm^2$, and the F_{OL} values were between 0.82 and $2.23\,J/cm^2$. The VSe_2 nanosheets displayed the lowest F_S and F_{OL} values of $0.05\,J/cm^2$ and $0.9\,J/cm^2$, respectively, which were much lower than that of the mainstream optical limiting materials, SnSe[24], graphene oxide ZnS (GOZS)[25], C_{60}[26], MoS_2[3], WS_2[3], graphene[3], CdS[27], and MWNTs[28], as compared in Fig. 5(b).

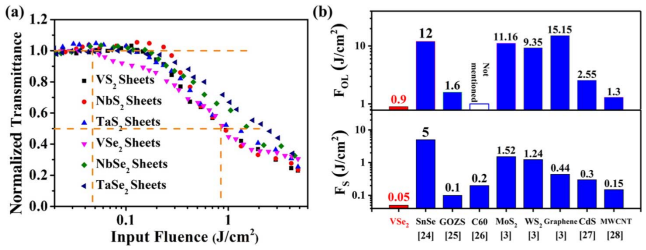

Fig. 5. (a) Relationship between the normalized transmittance of TMDs nanosheets and the input laser fluences. (b) Comparison of F_S and F_{OL} values for VSe_2 nanosheets in this work with other reported optical limiting materials at a laser wavelength of 532 nm.

Table 2. Linear Transmittance (T_0), Initial Threshold (F_S), and Optical Limiting Threshold (F_{OL}) of TMDs Nanosheets at 532 nm.

Materials	T_0 (%)	F_S (J·cm^{-2})	F_{OL} (J·cm^{-2})
VS_2	65	0.10	0.95
NbS_2	65	0.10	0.82
TaS_2	65	0.10	1.16
VSe_2	65	0.05	0.90
$NbSe_2$	65	0.08	1.53
$TaSe_2$	65	0.09	2.23

The nonlinear absorption coefficient (β) was used to further reveal the optical limiting mechanism in TMDs sheets. A model containing saturation and reverse saturation was applied to analyze the experimental results to obtain the β values. Using equations to fit the experimental results can get the β values. The obtained β values were further fitted to analyze the linearity between the β values and the incident laser energies to estimate the absorption methods[29–33]. As shown in Fig. S1 of Supplementary Materials, the linearity between the β values and irradiance intensity was calculated to be 88% for VS_2, 88% for NbS_2, 24% for TaS_2, 83% for VSe_2, 36% for $NbSe_2$, and 13% for $TaSe_2$, which indicated that both two-photon absorption (TPA) and reverse saturable absorption (RSA) existed in these samples. Besides, in order to explore the application potential of TMDs nanosheets in laser protection equipments and eliminate the influence of nonlinear scattering on optical limiting performance, NbS_2/PMMA and $NbSe_2$/PMMA composites were prepared to evaluate their optical limiting performance in solid state (in Fig. S2 of Supplementary Materials).

4. Conclusions

TMDs (VS_2, VSe_2, NbS_2, $NbSe_2$, TaS_2, and $TaSe_2$) in the VB group were successfully synthesized via solid state sintering, and the corresponding nanosheets were obtained by LPE. All of the tested TMDs nanosheets display satisfying optical limiting effects. The TMDs nanosheets possessed ultralow F_S (0.05–0.10 J/cm^2) and F_{OL} (0.82–2.23 J/cm^2) values, which surpassed the state-of-the-art MWNTs/C_{60}. In addition, the TMDs nanosheets displayed a normalized transmittance in the range of 20%–40% at the input energy of 1.28 GW/cm^2. This work opened up the potential of TMDs beyond MoS_2 in the optical limiting field.

Acknowledgement

This work was supported by the National Natural Science Foundation of China (No. 52002069), Natural Science Foundation of Fujian Province (No. 2020J05192), Opening Project of State Key Laboratory of Polymer Materials Engineering (Sichuan University) (No. sklpme2020-4-08), and State Key Laboratory of Materials Processing and Die & Mould Technology, Huazhong University of Science and Technology (No. P2021-024).

†These authors contributed equally to this work.

References

1. A. D. Piazza, C. Muller, K. Z. Hatsagortsyan, and C. H. Keitel, "Extremely high-intensity laser interactions with fundamental quantum systems," Rev. Mod. Phys. **84**, 1177 (2012).
2. J. Wang and W. J. Blau, "Inorganic and hybrid nanostructures for optical limiting," J. Opt. A: Pure Appl. Opt. **11**, 1464 (2009).
3. N. N. Dong, Y. X. Li, Y. Y. Feng, S. F. Zhang, X. Y. Zhang, C. X. Chang, J. T. Fan, L. Zhang, and J. Wang, "Optical limiting and theoretical modelling of layered transition metal dichalcogenide nanosheets," Sci. Rep. **5**, 14646 (2015).
4. L. L. Tao, H. Long, B. Zhou, S. F. Yu, S. P. Lau, Y. Chai, K. H. Fung, Y. H. Tsang, J. Q. Yao, and D. G. Xu, "Preparation and characterization of few-layer MoS_2 nanosheets and their good nonlinear optical responses in the PMMA matrix," Nanoscale **6**, 9713 (2014).
5. X. X. Liu, S. Y. Zhang, Z. Y. Yan, L. Guo, X. Y. Fan, F. Lou, M. R. Wang, P. Gao, G. G. Guo, T. Li, K. J. Yang, J. Li, and J. Q. Xu, "WSe_2 as a saturable absorber for a passively Q-switched Ho, Pr: LLF laser at 2.95 μm," Opt. Mater. Express **8**, 1213 (2018).
6. C. X. Zhang, H. Ouyang, R. L. Miao, Y. Z. Sui, H. Hao, Y. X. Tang, J. You, X. Zheng, Z. J. Xu, X. A. Cheng, and T. Jiang, "Anisotropic nonlinear optical properties of a SnSe flake and a novel perspective for the application of all-optical switching," Adv. Opt. Mater. **7**, 1900631 (2019).
7. G. W. Liang, L. L. Tao, Y. H. Tsang, L. H. Zeng, X. Liu, J. Li, J. Qu, and Q. Wen, "Optical limiting properties of few-layer MoS_2/PMMA composite under excitation of ultrafast laser pulses," J. Mater. Chem. C **7**, 495 (2020).
8. Q. Y. Ouyang, H. L. Yu, K. Zhang, and Y. J. Chen, "Saturable absorption and the changeover from saturable absorption to reverse saturable absorption of MoS_2 nanoflake array films," J. Mater. Chem. C **2**, 6319 (2014).
9. F. Gan, N. N. Dong, Z. W. Liu, J. Wang, and Y. Chen, "Organic small molecules covalently functionalized molybdenum disulfide hybrid material for optical limiting," Bull. Chem. Soc. Jpn. **93**, 26 (2019).
10. R. F. Wei, X. L. Tian, H. Zhang, Z. L. Hu, X. He, Z. Chen, Q. Q. Chen, and J. R. Qiu, "Facile synthesis of two-dimensional WS_2 with reverse saturable absorption and nonlinear refraction properties in the PMMA matrix," J. Alloys Compd. **684**, 224 (2016).
11. H. Long, L. L. Tao, C. P. Chiu, C. Y. Tang, K. H. Fung, Y. Chai, and Y. H. Tsang, "The WS_2 quantum dot: preparation, characterization and its optical limiting effect in polymethylmethacrylate," Nanotechnology **27**, 414005 (2016).

12. H. Long, L. L. Tao, C. Y. Tang, B. Zhou, Y. D. Zhao, L. H. Zeng, S. F. Yu, S. P. Lau, Y. Chai, and Y. H. Tsang, "Tuning nonlinear optical absorption properties of WS_2 nanosheets," Nanoscale **7**, 17771 (2015).
13. G. S. Liu, S. X. Dai, P. Li, B. H. Zhu, Z. K. Wu, and Y. Z. Gu, "Preparation and comparison of nonlinear optical properties of $MoSe_2$ with different types of structures," Opt. Mater. **95**, 109240 (2019).
14. C. J. Quan, M. He, C. He, Y. Y. Huang, L. P. Zhu, Z. H. Yao, X. Xu, C. H. Lu, and X. L. Xu, "Transition from saturable absorption to reverse saturable absorption in $MoTe_2$ nano-films with thickness and pump intensity," Appl. Surf. Sci. **457**, 115 (2018).
15. J. J. Wu, Y. R. Tao, L. Fan, Z. Y. Wu, X. C. Wu, and Y. Chun, "Visible light nonlinear absorption and optical limiting of ultrathin $ZrSe_3$ nanoflakes," Nanotechnology **27**, 465203 (2016).
16. J. J. Wu, Y. R. Tao, J. N. Wang, Z. Y. Wu, L. Fan, and X. C. Wu, "Reverse saturable absorption and nonlinear refraction of ultrathin ZrS_3 nanobelts," Nanoscale **8**, 10371 (2016).
17. S. J. Varma, J. Kumar, Y. Liu, K. Layne, J. J. Wu, C. L. Liang, Y. Nakanishi, A. Aliyan, W. Yang, P. M. Ajayan, and J. Thomas, "2D TiS_2 layers: a superior nonlinear optical limiting material," Adv. Opt. Mater. **5**, 1700713 (2017).
18. X. L. Zhang, Z. B. Liu, X. Q. Yan, X. C. Li, Y. S. Chen, and J. G. Tian, "Nonlinear optical and optical limiting properties of fullerene, multi-walled carbon nanotubes, graphene and their derivatives with oxygen-containing functional groups," J. Opt. **17**, 015501 (2015).
19. J. J. Wu, Y. R. Tao, X. C. Wu, and Y. Chun, "Nonlinear optical absorption of SnX_2 (X=S, Se) semiconductor nanosheets," J. Alloys Compd. **713**, 38 (2017).
20. M. Monisha, N. Priyadarshani, M. Durairaj, and T. C. S. Girisun, "2PA induced optical limiting behaviour of metal (Ni, Cu, Zn) niobate decorated reduced graphene oxide," Opt. Mater. **101**, 109775 (2020)
21. S. Bikorimana, P. Lama, A. Walser, R. Dorsinville, S. Anghel, A. MitiogluI, A. Micu, and L. Kulyuk, "Nonlinear optical responses in two-dimensional transition metal dichalcogenide multilayer: WS_2, WSe_2, MoS_2 and $Mo_{0.5}W_{0.5}S$," Opt. Express **24**, 20685 (2016).
22. S. Jeong, D. W. Yoo, J. T. Jang, M. Y. Kim, and J. W. Cheon, "Well-defined colloidal 2-D layered transition-metal chalcogenide nanocrystals via generalized synthetic protocols," J. Am. Chem. Soc. **134**, 18233 (2012).
23. J. N. Coleman, M. Lotya, A. O'Neill, S. D. Bergin, P. J. King, U. Khan, K. Young, A. Gaucher, S. De, R. J. Smith, I. V. Shvets, S. K. Arora, G. Stanton, H. Y. Kim, K. H. Lee, G. T. Kim, G. S. Duesberg, T. Hallam, J. J. Boland, J. J. Wang, J. F. Donegan, J. C. Grunlan, G. Moriarty, A. Shmeliov, R. J. Nicholls, J. M. Perkins, E. M. Grieveson, K. Theuwissen, D. W. McComb, P. D. Nellist, and V. Nicolosi, "Two-dimensional nanosheets produced by liquid exfoliation of layered materials," Science **331**, 568 (2011).
24. Y. T. Ye, Y. H. Xian, J. W. Cai, K. C. Lu, Z. Z. Liu, T. C. Shi, J. Du, Y. X. Leng, R. F. Wei, W. Q. Wang, X. F. Liu, G. Bi, and J. R. Qiu, "Linear and nonlinear optical properties of few-layer exfoliated SnSe nanosheets," Adv. Opt. Mater. **7**, 1800579 (2019).
25. P. L. Li, Y. H. Wang, M. Shang, L. F. Wu, and X. X. Yu, "Enhanced optical limiting properties of graphene oxide-ZnS nanoparticles composites," Carbon **142**, 1 (2019).
26. K. P. Wang, X. Y. Zhang, I. M. Kislyakov, N. N. Dong, S. F. Zhang, G. Z. Wang, J. T. Fan, X. Zou, J. Du, Y. X. Leng, Q. Z. Zhao, K. Wu, J. P. Chen, S. M. Baesman, K. S. Liao, S. Maharjan, H. Z. Zhang, L. Zhang, S. A. Curran, R. S. Oremland, W. J. Blau, and J. Wang, "Bacterially synthesized tellurium nanostructures for broadband ultrafast nonlinear optical applications," Nat. Commun. **10**, 3985 (2019).
27. M. Feng, R. Q. Sun, H. B. Zhan, and Y. Chen, "Decoration of carbon nanotubes with CdS nanoparticles by polythiophene interlinking for optical limiting enhancement," Carbon **48**, 1177 (2010).
28. K. P. Loh, H. Zhang, W. Z. Chen, and W. Ji, "Templated deposition of MoS_2 nanotubules using single source precursor and studies of their optical limiting properties," J. Phys. Chem. B **110**, 1235 (2006).
29. N. Dong, Y. Li, S. Zhang, N. McEvoy, R. Gatensby, G. S. Duesberg, and J. Wang, "Saturation of two-photon absorption in layered transition metal dichalcogenides: experiment and theory," ACS Photon. **5**, 1558 (2018).
30. S. Zhang, N. Dong, N. McEvoy, M. O'Brien, S. Winters, N. C. Berner, C. Yim, Y. Li, X. Zhang, Z. Chen, L. Zhang, G. S. Duesberg, and J. Wang, "Direct observation of degenerate two-photon absorption and its saturation in WS_2 and MoS_2 monolayer and few-layer films," ACS Nano **9**, 7142 (2015).
31. L. Tao, H. Long, B. Zhou, S. F. Yu, S. P. Lau, Y. Chai, K. H. Fung, Y. H. Tsang, J. Yao, and D. Xu, "Preparation and characterization of few-layer MoS_2 nanosheets and their good nonlinear optical responses in the PMMA matrix," Nanoscale **6**, 9713 (2014).
32. S. J. Hua, K. Du, H. Wang, W. D. Zhang, and E. Dogheche, "Affirming nonlinear optical coefficient constancy from z-scan measurement," Chin. Opt. Lett. **18**, 071903 (2020).
33. M. Y. Shubar, H. L. Saadon, and S. J. Abbas, "Nonlinear optical switching and all-figures of merit in $Bi_2S_{3-x}Se_x$/PMMA nanocomposite films investigated by Z scan under visible CW laser," Chin. Opt. Lett. **18**, 011902 (2020).